

This is a post-peer-review, pre-copyedit version of an article published in Planta. The final authenticated version is available online at: <http://dx.doi.org/10.1007/s00425-017-2774-9>

Chemical characterization and identification of Pinaceae pollen by infrared microspectroscopy

Boris Zimmermann

Faculty of Science and Technology, Norwegian University of Life Sciences

Drøbakveien 31, 1432 Ås, Norway.

Tel: + +47 9751 1114

Fax: +47 6723 0691

E-mail: boris.zimmermann@nmbu.no

Main conclusion:

FTIR microspectroscopy, in combination with spectral averaging procedure, enables precise analysis of pollen grains for chemical characterization and identification studies of fresh and fossilised pollen in botany, ecology and palaeosciences.

Abstract

Infrared microspectroscopy (μ FTIR) of Pinaceae pollen can provide valuable information on plant phenology, ecophysiology and paleoecology, but measurements are challenging, resulting in unreproducible spectra. The comparative analysis of μ FTIR spectra belonging to morphologically different Pinaceae pollen, namely bisaccate *Pinus* and monosaccate *Tsuga* pollen, was conducted. The study shows that the main cause of spectral variability is non-radial symmetry of bisaccate pollen grains, while additional variation is caused by Mie scattering. Averaging over relatively small number of single pollen grain spectra (approx. 5-10) results with reproducible data on pollen chemical composition. The practical applicability of the μ FTIR spectral averaging method has been demonstrated by the partial least squares regression-based differentiation of the two closely related *Pinus* species with morphologically indistinguishable pollen: *Pinus mugo* (mountain pine) and *Pinus sylvestris* (Scots pine). The study has demonstrated that the μ FTIR approach can be used for identification, differentiation and chemical characterization of pollen with complex morphology. The methodology enables analysis of fresh pollen, as well as fossil pollen from sediment core samples, and can be used in botany, ecology and paleoecology for study of biotic and abiotic effects on plants.

Keywords: Fourier transform infrared spectroscopy, Mie scattering, Multivariate analysis, *Pinus mugo*, *Pinus sylvestris*, *Tsuga canadensis*

Introduction

Pinaceae are one of the most ecologically important plant family with widespread range, in particular considering boreal, costal and mountain forests of the Northern Hemisphere. Moreover, members of the family are widely cultivated for softwood timber and pulpwood, and thus are of greatest economic importance. In general, Pinaceae species have relatively rich fossil record that indicates appearance of Pinaceae ancestors more than 200 million years ago, with diversification of the family during Jurassic and Cretaceous periods (Miller 1999). Fossil pollen grains are often not only the most abundant but also among the best preserved remains of Pinaceae species, thus providing crucial information for the reconstruction of past flora, population sizes and terrestrial communities (Lindbladh et al. 2002). In addition, fresh pollen can provide valuable information on plant phenology, ecophysiology, population dynamics and gene flow (Yazdani et al. 1989; Savolainen et al. 2007).

Pollen analysis is usually based on morphology since pollen can have well preserved form and structure for millions of years, with specific shape, size and texture that are unique for plant taxa (Hesse 2009). Pinaceae are described as saccate pollen due to a large hollow projection (saccus) from the central body of pollen grain. Most of the Pinaceae species, such as *Pinus*, *Abies*, *Picea*, *Cedrus* and *Podocarpus*, have bisaccate pollen, with two laterally-placed sacci (Hesse 2009). In addition to morphometric analysis, chemical analysis of pollen can provide valuable information as well. Pollen wall is generally comprised of an inner layer (intine), an outer layer (exine), and a cover layer (pollen coat). Pollen wall has not only complex surface morphology but also complex and distinct chemical components. Biochemistry of these components depends on a number of metabolic events, involving for example lipid and polysaccharide metabolisms (Pacini and Hesse 2005; Blackmore et al. 2007; Souza et al. 2009; Ariizumi and Toriyama 2011; Jiang et al. 2013; Shi et al. 2015). The most important component of the outer layer of the pollen grain wall (exine) are sporopollenins, an extremely resilient and chemically stable group of compounds that preserves pollen for long periods of time (Bedinger 1992). Sporopollenins are complex biopolymers composed of polyhydroxylated unbranched aliphatic and phenolic constituents (Kim and Douglas 2013), and they are the predominant chemical components of Pinaceae saccus. Sporopollenin phenolic constituents (i.e. phenylpropanoids) serve as protective absorbing screens of solar UV radiation, and, as a result, concentration and composition of phenylpropanoids in pollen grain wall is wavelength-dependent. Therefore, measurement of phenylpropanoids can be used as UV-B proxy, allowing assessment of changes in the flux of UV-B radiation over geological time (Rozema et al. 2001; Watson et al. 2007; Willis et al. 2011; Lomax et al. 2012).

In general, chemical composition of pollen is of importance in order to determine the principal structural, nutritious and metabolic components. For example, triglyceride lipids primarily serve as carbon and long-term energy reserves in a form of lipid bodies, while phospholipids serve as structural components in cell membranes (Piffanelli et al. 1998; Zhang et al. 2016). Carbohydrates, in the form of cytoplasmic saccharides, have a vital function in the resistance to dehydration and temperature stress, as well as serving as cell wall components and energy reserves (Pacini 1996; Speranza et al. 1997). Proteins have both a structural and a functional role, with crucial functions in signalling and interactions of organisms with environment (Roulston et al. 2000; Holmes-Davis et al. 2005). A number of studies have demonstrated the importance of precise measurement of pollen chemical composition (Vanherpen 1981; Vesprini et al. 2002; Lahlali et al. 2014). Unfortunately, measurement of chemical composition of pollen, such as measurements of proteins (Roulston et al. 2000), carbohydrates (Speranza et al. 1997), and lipids (Piffanelli et al. 1998), are rarely conducted since they require complex sample preparation and laborious analysis. During the recent years, a number of techniques, such as laser induced breakdown spectroscopy (LIBS) (Boyain-Goitia et al. 2003), matrix assisted laser desorption ionization mass spectrometry (MALDI-MS) (Liang et al. 2013; Seifert et al. 2015; Joester et al. 2016; Seifert et al. 2016), thermally assisted hydrolysis and methylation pyrolysis gas chromatography/mass spectrometry (THM-py-GC/MS) (Blokker et al. 2005; Watson et al. 2007; Lomax et al. 2008; Willis et al. 2011),

and Raman spectroscopy (Boyain-Goitia et al. 2003; Pummer et al. 2013; Joester et al. 2016; Seifert et al. 2016), have been introduced for the chemical characterization of pollen grains.

In the last decade, analysis of pollen by Fourier transform infrared (FTIR) spectroscopy has seen rapid development in the field of botany and palynology (Pappas et al. 2003; Gottardini et al. 2007; Dell'Anna et al. 2009; Zimmermann 2010; Parodi et al. 2013; Pummer et al. 2013; Lahlali et al. 2014; Zimmermann and Kohler 2014; Bağcıoğlu et al. 2015; Jiang et al. 2015; Zimmermann et al. 2015a; Zimmermann et al. 2015b; Julier et al. 2016; Zimmermann et al. 2016; Bağcıoğlu et al. 2017; Jardine et al. 2017). A major advantage of FTIR spectroscopy is fast and economical measurement of pollen samples which can be conducted without any chemical pre-treatment. In general, FTIR spectra of pollen contain vibrational frequencies of molecular bonds that can be directly related to molecular functional groups of chemical constituents (Pappas et al. 2003; Gottardini et al. 2007; Zimmermann 2010; Zimmermann and Kohler 2014). Given that FTIR spectroscopy is based on the spectral measurement of many different spectral cellular features, the resulting spectrum is a fingerprint of the overall chemical composition of a pollen sample, and not just one type of chemicals. For example, main biochemical constituents of pollen, such as lipids, proteins, and carbohydrates can be easily identified based on their specific infrared signals (Bağcıoğlu et al. 2015; Jiang et al. 2015; Zimmermann et al. 2015b; Jardine et al. 2017). This property enables measurement of structural changes at molecular level, such as phase transition behaviour of lipids (Sowa et al. 1991) and estimation of different protein secondary structures in pollen grains (Sowa et al. 1991; Wolkers and Hoekstra 1995; Lahlali et al. 2014; Depciuch et al. 2017). Furthermore, even chemistry of complex compounds, such as sporopollenins in both pollen and plant spores, has been studied extensively by FTIR (Dominguez et al. 1999; Yule et al. 2000; Watson et al. 2007; Fraser et al. 2012; Lomax et al. 2012; Fraser et al. 2014; Bağcıoğlu et al. 2015; Lomax and Fraser 2015; Zimmermann et al. 2015a; Jardine et al. 2016). Accurate measurement of sporopollenin by FTIR enables, for example, quantification of phenylpropanoids by a non-destructive approach (Watson et al. 2007; Fraser et al. 2011; Jardine et al. 2016; Jardine et al. 2017). A number of studies have demonstrated that FTIR spectra of pollen enable detailed chemical analysis for identification and classification purposes (Pappas et al. 2003; Gottardini et al. 2007; Dell'Anna et al. 2009; Zimmermann 2010; Julier et al. 2016; Zimmermann et al. 2016; Bağcıoğlu et al. 2017). Moreover, FTIR spectroscopy is a valuable method for pollen phenotyping since it provides assessment of environmental effects, such as temperature stress (Lahlali et al. 2014; Zimmermann and Kohler 2014; Jiang et al. 2015) or anthropogenic pollution stress (Depciuch et al. 2016; Depciuch et al. 2017).

Although FTIR microspectroscopy (μ FTIR) enables measurement of a single pollen grain, the measurement is quite challenging, resulting in unreproducible spectra, thus severely hindering application of this method in paleoecology (Dell'Anna et al. 2009; Bağcıoğlu et al. 2015; Lukacs et al. 2015; Zimmermann et al. 2015a; Zimmermann et al. 2016). In general, μ FTIR of pollen is hindered by strong Mie scattering, since pollen grains, due to size and shape, are highly scattering samples in the infrared (Lukacs et al. 2015; Zimmermann et al. 2015a). The strong light scattering results in anomalous spectral features that can significantly interfere with and distort the signals of chemical absorption. Pollen grains within the range of 5-25 μ m show the strongest scattering anomalies, since the sizes are exactly within the magnitude of the mid-IR light (Zimmermann et al. 2015a). For such samples, the conventional measurement on microscope slides is not feasible and different experimental setting needs to be applied, such as embedding in a soft paraffin layer between two sheets of polyethylene foils (Zimmermann et al. 2016). Although grains larger than 40 μ m do not show strong scattering and can be measured in conventional way, Pinaceae grains are exception due to complex structure with non-radial symmetry (Bağcıoğlu et al. 2015; Zimmermann et al. 2015a). In addition to the scattering issues, single-grain FTIR spectra of bisaccate Pinaceae pollen have high spectral variability due to differences in chemical absorption bands (Zimmermann et al. 2015a). More precisely, bilateral symmetry of pollen causes distinctive and noninvariant spatial orientations, resulting in high variability of corresponding FTIR spectra (Zimmermann et al. 2015a).

In this study, averaging of μ FTIR single-grain pollen spectra was employed in order to obtain reproducible chemical fingerprints for characterisation, identification and differentiation of Pinaceae pollen

species. The practical applicability of the μ FTIR spectral averaging method was evaluated by measurement and differentiation of the two pine species: *Pinus mugo* (mountain pine) and *Pinus sylvestris* (Scots pine). Although *P. mugo* and *P. sylvestris* can be differentiated based on quantitative and qualitative characters of tree (sporophyte) phenotypes (Christensen and Dar 1997), there is a considerable overlap in their pollen (gametophyte) morphology, and clear morphological criteria for differentiating pollen of the two species are still lacking (Klaus 1978; Bykowska and Klimko 2015). Therefore, the two pine species represent challenging experimental pollen set for μ FTIR-based differentiation study. In addition, the study has included *Tsuga canadensis* (eastern hemlock) pollen samples. *T. canadensis* has monosaccate pollen grains with spherical symmetry, thus it represents good referent sample to morphologically different (Ho and Sziklai 1972; Nakagawa et al. 2000), but chemically quite similar (Zimmermann 2010), bisaccate *P. mugo* and *P. sylvestris*.

Materials and methods

Samples

Six pollen samples were collected in 2014 from six different Pinaceae individuals (i.e. parental lineages) growing at campus area of Norwegian University of Life Sciences (Ås, Norway). Two pollen samples per each of the three Pinaceae species were measured: *Pinus sylvestris* L., *Pinus mugo* Turra and *Tsuga canadensis* (L.) Carrière. Each pollen sample was collected from at least ten pollen strobili (male flowers) on one individual Pinaceae tree. Pollen were collected immediately following cone opening and sporangial sac dehiscence. The pollen samples were kept at room temperature for 24 hours, and subsequently stored at -15°C until the μ FTIR measurements.

Measurement

Microscopic transmission measurements of pollen were performed using a Vertex 70 FTIR spectrometer with a Hyperion 3000 IR microscope (Bruker Optik, Ettlingen Germany), equipped with a global mid-IR source and a liquid nitrogen-cooled mercury cadmium telluride (MCT) detector. The pollen samples were deposited onto 1 mm thick zinc selenide (ZnSe) optical windows without any chemical pretreatment. The spectra were recorded with a total of 64 scans in the $4000\text{--}600\text{ cm}^{-1}$ spectral range, with a spectral resolution of 4 cm^{-1} . Samples were measured using $15\times$ objective, with 50×50 aperture size. Background (reference) spectra were recorded at the start of measurements (one per sample measurement) by measuring empty areas of ZnSe slides. Visible images of the measured pollen grains were obtained by a charge coupled device (CCD) camera coupled to the microscope. The microscope was equipped with a computer-controlled x/y/z stage. The spectroscopic system was controlled with OPUS 7.5 software (Bruker Optik). Six pollen samples were measured, and 200 spectra per sample were obtained, each corresponding to a different single pollen grains, resulting in 1200 μ FTIR spectra of single pollen grains in total.

Data analysis

For the analysis of spectral set, spectral region of $1900\text{ to }800\text{ cm}^{-1}$ was selected. Prior to analysis, bands belonging to gaseous H_2O and CO_2 from ambient air were removed from the spectra by using the OPUS Atmospheric Compensation command in OPUS 7.5. Furthermore, spectra were smoothed and transformed to second derivative form by Savitzky-Golay (SG) algorithm using a polynomial of power 2 with window size 15. After derivation by SG algorithm, spectra were processed using extended multiplicative signal correction (EMSC) with linear, quadratic and cubic component. The SG algorithm was used to enhance spectral features, while the EMSC pre-processing was employed for the normalization and for the separation of chemical and physical variations in vibrational spectra, including the baseline correction (Zimmermann and Kohler 2013). The selection of pre-processing parameters was based on suppressing noise while enhancing intensity of broad amide bands in the $1650\text{--}1520\text{ cm}^{-1}$ region, as explained in detail in our previous study (Zimmermann and

Kohler 2013). The Kolmogorov-Smirnov test was applied to assess whether intensity values of pre-processed spectra for each number followed a normal distribution.

Following the spectral pre-processing, three additional sets of spectra were generated by calculating average spectrum of 5, 10 and 20 single pollen grain spectra. Thus calculated average spectra were normalized by using multiplicative signal correction (MSC) for each set of average spectra separately. The spectral set with pre-processed single pollen grain spectra, as well as the three additional spectral sets comprising average spectra, were used in the data analyses.

Biochemical similarities between pollen samples were estimated by using principal component analysis (PCA) and variability test based on Pearson correlation coefficients (PCC). The PCC was calculated for the whole selected spectral region, from 1900 to 800 cm^{-1} . The Kruskal-Wallis and Mann-Whitney U tests were used to calculate the statistical significance of differences in the PCA principal component scores between species. In addition, partial least-squares regression (PLSR) was used to evaluate classification, either between Pinaceae genera (*Pinus* and *Tsuga*) or between *Pinus* species (*P. sylvestris* and *P. mugo*). The optimal number of components (i.e. PLSR factors) of the calibration models (A_{Opt}) was determined using segmented cross-validation using ten segments. The PLSR coefficient of determination (R^2) between the taxa was used to evaluate the calibration models. All pre-processing methods and data analyses were performed using The Unscrambler X 10.3 (CAMO Software, Oslo, Norway), as well as functions and in-house developed routines written in MATLAB 2014a. 8.3.0.532 (The MathWorks, Natick, Massachusetts, USA).

Results

Morphology of the Pinaceae pollen samples

The optical microscope images of pollen species reveal clear morphological differences between *Pinus* and *Tsuga* pollen grains (Fig. 1). The two laterally-placed sacci of bisaccate *Pinus* pollen are giving this type of pollen two bilateral planes of symmetry, both perpendicular to each other and to the equatorial plane. On the other hand, *T. canadensis* pollen grain is monosaccate, with equatorial saccus (i.e. frill or fringe), giving this type of pollen distinctive biconvex circular symmetry. It should be mentioned that *T. canadensis* pollen has an additional bilateral symmetry perpendicular to the circular axis. However, this symmetry can be disregarded since, due to density and geometric constraints, *T. canadensis* pollen will have overwhelming tendency to be orientated in a polar view on a measuring slide.

Spectral differences between pollen genera and species

The μFTIR spectra of single pollen grains belonging to the two *Pinus* species have high variability due to the aforementioned variability of spatial orientations on μFTIR slides, caused by bilateral symmetry of the pollen grains (Fig. 2). For instance, the spectrum of the pollen grain that has distal polar orientation has predominant contribution of saccus region, with strong signals of sporopollenin-related phenylpropanoids (Fig. 2a). On the other hand, the spectrum of the pollen grain that has equatorial profile orientation has predominant contribution of corpus region, with strong signals of lipids and proteins (Fig. 2b). In addition, the differences between the two spectra are due to the scattering artefacts, in particular in the low-wavelength spectral region ($< 1000 \text{ cm}^{-1}$).

Contrary to the single grain μFTIR spectra of the two *Pinus* species, spectra of *T. canadensis* pollen are quite invariant (Figs. 2c and 2d). Due to spherical symmetry, with large length difference between polar and equatorial axes, *Tsuga canadensis* pollen grains have consistent spatial orientation on μFTIR slides with almost exclusively polar orientation.

The low reproducibility (i.e. high variability) of the measured μFTIR spectra of *Pinus*, when compared with the spectra of *Tsuga*, can be seen in the PCA score plot in Fig.3. However, it is apparent that the variability is non-random and is significantly species-based. As no wavenumber was found to be normally distributed (according to the Kolmogorov-Smirnov test; Table S1 in the Supplementary material), the Kruskal-Wallis and

Mann-Whitney U tests were used to calculate the statistical significance of differences in the PCA principal component scores between pollen species (Table S2 in the Supplementary material). The statistical analyses, based on the PC scores, clearly show that μ FTIR spectra of pollen species are significantly different (P -values < 0.0001).

The Pearson Correlation Coefficient (PCC), expressed as 1-PCC, was used to estimate the spectral variability of pollen samples (Table 1). The PCC measures correlation between variables, where a value of 1 indicates high positive correlation. Therefore, small variability is indicated by small 1-PCC values. It is apparent that the variability of bisaccate grains of *Pinus* with bilateral symmetry is considerably higher than variability of monosaccate grains of *Tsuga* with radial symmetry.

Spectral averaging and differentiation of pollen species

In order to compensate variability due to spatial orientation of the grains, a new set of spectra were created, where each new spectrum was an average of either 5, 10 or 20 single grain spectra. The PCA and PLSR results (Fig. 4 and Table 2), as well as the statistical analyses (Tables S2 and S3 in the Supplementary material), show that the average spectra have high reproducibility and enable characterization, identification and differentiation of pollen samples.

The PLSR model based on discrimination of single pollen grains has relatively high discrimination power, with $R^2 = 0.88$ (Table 2). However, the PLSR model has relatively high optimal number of components ($A_{Opt} = 11$) with probable over-fitting result, since the regression coefficient shows strong contribution of noise and artefacts, such as white noise, water vapour, and Mie scattering (Fig. 5). In general, PLSR models are greatly improved by spectral averaging, with $R^2 > 0.95$, and considerably lower optimal number of components ($A_{Opt} \approx 5$), even when averaging is based on only five grains. In order to avoid an overly-optimistic estimate of discrimination power, PLSR models with fewer factors were preferred. For example, the PLSR model based on 10 grain average ($R^2 = 0.96$) has considerably higher discrimination power than the model based on discrimination of single pollen grains ($R^2 = 0.83$), provided that the number of components is the same ($A = 4$; Table 2). The separation between the two *Pinus* species is based predominantly on signals belonging to lipids (1740 cm^{-1} , C=O stretch; 1475 cm^{-1} , CH_2 bending), proteins (1650 , amide I: C=O stretch; 1550 , amide II: NH deformation and C-N stretch), and sporopollenins (1622 , 1517 and 833 cm^{-1} , all bands related to phenylpropanoids building blocks) (Fig. 5) (Zimmermann 2010; Bağcıoğlu et al. 2015).

Discussion

Automated and objective analysis of samples is a persistent problem in palynology (Holt and Bennett 2014). In this study, a highly challenging pollen samples, covering two closely related pine species of high economic and ecological importance, have been chosen for μ FTIR analysis. *P. mugo* and *P. sylvestris*, are highly variable species showing wide range of morphological and physiological characteristics as well as adaptive traits for specific environments. *P. sylvestris* has the largest geographical distribution of all pines, covering the whole Europe, from the Mediterranean to well within the Arctic Circle, while *P. mugo* is a predominantly high-altitude species with restricted spread across south and central European mountain ranges (Wachowiak et al. 2011; Wachowiak et al. 2015). Genetic studies have shown that *P. mugo* and *P. sylvestris* share similar genetic background, indicating divergence in recent evolutionary past (Wachowiak et al. 2011; Wachowiak et al. 2015). Moreover, hybrids of the two species (*P. mugo* \times *sylvestris*) are relatively widespread in natural populations since the parent plants readily undergo spontaneous hybridization in the autochthonous populations (Staszkie.J and Tyszkiew.M 1969; Christensen 1987; Christensen and Dar 1997; Wachowiak et al. 2011). Interspecific gene flow and high morphological polymorphism causes serious taxonomic problems, in particular regarding *P. mugo* (Christensen 1987; Businsky and Kirschner 2006; Wachowiak et al. 2011; Boratynska et al. 2015). In this study, pollen samples were obtained from *P. mugo* subsp. *mughus* (*P. mugo* sensu stricto), a polycormic shrub subspecies with prostrate growth.

In general, morphometric analysis enables taxonomic determination of *Pinus* pollen grains at the level of the *Strobilus* and *Pinus* subgenera, due to the difference in outline of the sacci in polar view (Bykowska and Klimko 2015). However, differentiation at species level is extremely challenging and requires detailed analysis by scanning electron microscopy (Nakagawa et al. 2000). Concerning interspecific gene flow between *P. sylvestris* and *P. mugo*, with widespread hybridization, it is reasonable that the two species lack morphological features for pollen differentiation (Klaus 1978; Bykowska and Klimko 2015).

Spectral differences between pollen genera and species

The μ FTIR spectra of single pollen grains belonging to *Pinus mugo* and *Pinus sylvestris* have relatively high variability, compared to *Tsuga canadensis* spectra, due to bilateral symmetry of bisaccate pollen grains of *Pinus* (Fig. 2). The high variability of the μ FTIR spectra of the two *Pinus* pollen species is consistent with the results of our previous studies on bisaccate pollen of *Pinus*, *Picea*, *Cedrus*, *Abies* and *Podocarpus* (Bağcıoğlu et al. 2015; Zimmermann et al. 2015a). Due to spherical symmetry of monosaccate pollen grains, *T. canadensis* spectra are relatively invariant. It should be noted that all three studied species have relatively similar chemical composition of pollen (Zimmermann 2010). Therefore, the comparative study between *Pinus* and *Tsuga* samples shows that the majority of spectral variation originates due to either spatial orientation on microscope slides or scattering on substructures of bisaccate pollen grains.

The previous study has demonstrated that differentiation of congeneric species of pollen with radial symmetry can be obtained by μ FTIR spectroscopy (Zimmermann et al. 2016). Here, it has been demonstrated that congeneric species of pollen with bilateral symmetry can be differentiated as well. In this respect, the presented averaging μ FTIR methodology is more similar to multigrain μ FTIR measurements (Dell'Anna et al. 2009; Bağcıoğlu et al. 2015; Julier et al. 2016), than to single grain μ FTIR measurements (Zimmermann et al. 2016).

Application of μ FTIR approach

It should be noted that certain variation in chemical composition between pollen grains of the same parental (sporophytic) lineage is always present, due to genetic differences between the pollen grains. Chemical composition of pollen depends both on sporophytic (usually diploid) genome which controls development of exine and pollen coat, as well as gametophytic (usually haploid) genome which controls development of intracellular materials and inner layer of pollen grain wall (intine) (Piffanelli et al. 1998; Jiang et al. 2013). The vast majority of μ FTIR spectral signals are related to the intracellular structures, such as lipid and carbohydrate nutrients synthesized in the vegetative cell of the pollen grain under the control of the gametophytic genome. Unfortunately, spectral averaging reduces these chemical differences between individual pollen grains, resulting in an average μ FTIR spectra of a pollen population.

Although μ FTIR approach is limited regarding precise chemical characterization of a single grain bisaccate pollen, it can still have broad application. For example, the spectral averaging methodology enables measurement of chemical variation between pollen samples originating from different strobili or branches of an individual sporophyte, thus local biotic and abiotic effects on pollen can be studied, such as influence of pathogens, pollution or partial shading. Likewise, the presented FTIR methodology enables analysis of pollen grains from sediment core samples, thus providing chemical characterization of a stratigraphic sequence of pollen.

Moreover, chemical information of pollen obtained by this methodology can be combined with the results of other multigrain-based methods, such as THM-py-GC/MS (Blokker et al. 2005; Watson et al. 2007; Lomax et al. 2008; Willis et al. 2011) and MALDI-MS (Liang et al. 2013; Seifert et al. 2015; Seifert et al. 2016), in order to obtain comprehensive chemical fingerprints of pollen species and ecotypes. Regarding pollen grain wall chemistry, FTIR analysis of pollen cannot yet provide the same level of quantitative and qualitative chemical analysis of sporopollenins as THM-py-GC/MS. However, it is reasonable to assume that methodology will significantly improve in future by combining FTIR spectroscopy with chemometrics of multivariate

regression, as was the case for other complex biological samples (Zimmermann and Kohler 2013). This has already been indicated in a UV irradiance study where phenylpropanoid estimates were based on FTIR measurements of *Lycopodium* spores from a natural shading gradient (Jardine et al. 2017). It should be taken into account that a typical THM-py-GC/MS measurements of phenylpropanoids in *Pinus* pollen is conducted on approx. 50 pollen grains (Willis et al. 2011), while this study has demonstrated that reproducible chemical fingerprint of pollen can be obtained from even smaller number of pollen grains (5-20). Furthermore, FTIR measurements are non-destructive and thus can provide additional level of chemical information, such as lipid and protein secondary structure (Sowa et al. 1991; Wolkers and Hoekstra 1995; Lahlali et al. 2014; Depciuch et al. 2017), which cannot be obtained by destructive mass spectrometry approaches. Finally, chemical analysis of pollen samples by μ FTIR, combined with DNA sequencing from single pollen grain (Parducci et al. 2005; Nakazawa et al. 2013), could provide valuable information in paleoecology for reconstruction of past communities, environments, and plant-environment interactions.

Conclusions

Comparative analysis of μ FTIR spectra belonging to morphologically different Pinaceae pollen, namely bisaccate *Pinus* and monosaccate *Tsuga* pollen, proves that the main cause of spectral variability is non-radial symmetry of bisaccate pollen grains. The spectral effects due to pollen grain spatial orientation on microscope slide, as well as scattering effects, can be considerably reduced by spectral averaging approach. Moreover, the value of the μ FTIR methodology has been demonstrated on the two closely related *Pinus* species with morphologically indistinguishable pollen. The spectral averaging over relatively small number of single pollen grain spectra results in high spectral reproducibility as shown by the PCC. The reliable PLSR models, with high discrimination power ($R^2 > 0.95$) and clear chemical fingerprints, were obtained for differentiation of *P. sylvestris* and *P. mugo* pollen. Therefore, the study has demonstrated that the μ FTIR approach can be used for identification, differentiation and chemical characterization of Pinaceae pollen and other pollen species with non-radial symmetry.

Supplementary material

Additional Supplementary material may be found in the online version of this article at the publisher's website.

Acknowledgements

The research was supported by the European Commission through the Seventh Framework Programme (FP7-PEOPLE-2012-IEF project no. 328289). The author thanks M. Furlan Zimmermann.

References

- Ariizumi T, Toriyama K (2011) Genetic Regulation of Sporopollenin Synthesis and Pollen Exine Development. *Annu Rev Plant Biol* 62:437-460. doi:10.1146/annurev-arplant-042809-112312
- Bağcıoğlu M, Kohler A, Seifert S, Kneipp J, Zimmermann B (2017) Monitoring of plant–environment interactions by high-throughput FTIR spectroscopy of pollen. *Methods in Ecology and Evolution* 8 (7):870-880. doi:10.1111/2041-210X.12697
- Bağcıoğlu M, Zimmermann B, Kohler A (2015) A Multiscale Vibrational Spectroscopic Approach for Identification and Biochemical Characterization of Pollen. *Plos One* 10 (9). doi:ARTN e0137899 10.1371/journal.pone.0137899
- Bedinger P (1992) The Remarkable Biology of Pollen. *Plant Cell* 4 (8):879-887. doi:DOI 10.1105/tpc.4.8.879

- Blackmore S, Wortley AH, Skvarla JJ, Rowley JR (2007) Pollen wall development in flowering plants. *New Phytologist* 174 (3):483-498. doi:10.1111/j.1469-8137.2007.02060.x
- Blokker P, Yeloff D, Boelen P, Broekman RA, Rozema J (2005) Development of a proxy for past surface UV-B irradiation: A thermally assisted hydrolysis and methylation py-GC/MS method for the analysis of pollen and spores. *Anal Chem* 77 (18):6026-6031. doi:10.1021/ac050696k
- Boratynska K, Jasinska AK, Boratynski A (2015) Taxonomic and geographic differentiation of *Pinus mugo* complex on the needle characteristics. *Syst Biodivers* 13 (6):901-915. doi:10.1080/14772000.2015.1058300
- Boyain-Goitia AR, Beddows DCS, Griffiths BC, Telle HH (2003) Single-pollen analysis by laser-induced breakdown spectroscopy and Raman microscopy. *Applied Optics* 42 (30):6119-6132. doi:10.1364/Ao.42.006119
- Businsky R, Kirschner J (2006) Nomenclatural notes on the *Pinus mugo* complex in Central Europe. *Phyton-Ann Rei Bot A* 46 (1):129-139
- Bykowska J, Klimko M (2015) Pollen Morphology of *Pinus Mugo Turra* X *Pinus Sylvestris* L. Hybrids and Parental Species in an Experimental Culture. *Acta Biol Cracov Bot* 57 (1):149-160. doi:10.1515/abscb-2015-0009
- Christensen KI (1987) Taxonomic Revision of the *Pinus-Mugo* Complex and *Pxrhaetica* (*Pxrhaetica-Mugoxylvestris*) (Pinaceae). *Nord J Bot* 7 (4):383-408. doi:DOI 10.1111/j.1756-1051.1987.tb00958.x
- Christensen KI, Dar GH (1997) A morphometric analysis of spontaneous and artificial hybrids of *Pinus mugo* x *sylvestris* (Pinaceae). *Nord J Bot* 17 (1):77-86. doi:DOI 10.1111/j.1756-1051.1997.tb00291.x
- Dell'Anna R, Lazzeri P, Frisanco M, Monti F, Malvezzi Campeggi F, Gottardini E, Bersani M (2009) Pollen discrimination and classification by Fourier transform infrared (FT-IR) microspectroscopy and machine learning. *Analytical and bioanalytical chemistry* 394 (5):1443-1452. doi:10.1007/s00216-009-2794-9
- Depciuch J, Kasprzyk I, Roga E, Parlinska-Wojtan M (2016) Analysis of morphological and molecular composition changes in allergenic *Artemisia vulgaris* L. pollen under traffic pollution using SEM and FTIR spectroscopy. *Environ Sci Pollut R* 23 (22):23203-23214. doi:10.1007/s11356-016-7554-8
- Depciuch J, Kasprzyk I, Sadik O, Parlinska-Wojtan M (2017) FTIR analysis of molecular composition changes in hazel pollen from unpolluted and urbanized areas. *Aerobiologia* 33 (1):1-12. doi:10.1007/s10453-016-9445-3
- Dominguez E, Mercado JA, Quesada MA, Heredia A (1999) Pollen sporopollenin: degradation and structural elucidation. *Sex Plant Reprod* 12 (3):171-178. doi:DOI 10.1007/s004970050189
- Fraser WT, Scott AC, Forbes AES, Glasspool IJ, Plotnick RE, Kenig F, Lomax BH (2012) Evolutionary stasis of sporopollenin biochemistry revealed by unaltered Pennsylvanian spores. *New Phytologist* 196 (2):397-401. doi:10.1111/j.1469-8137.2012.04301.x
- Fraser WT, Sephton MA, Watson JS, Self S, Lomax BH, James DI, Wellman CH, Callaghan TV, Beerling DJ (2011) UV-B absorbing pigments in spores: biochemical responses to shade in a high-latitude birch forest and implications for sporopollenin-based proxies of past environmental change. *Polar Res* 30. doi:ARTN 8312
10.3402/polar.v30i0.8312
- Fraser WT, Watson JS, Sephton MA, Lomax BH, Harrington G, Gosling WD, Self S (2014) Changes in spore chemistry and appearance with increasing maturity. *Rev Palaeobot Palyno* 201:41-46. doi:10.1016/j.revpalbo.2013.11.001
- Gottardini E, Rossi S, Cristofolini F, Benedetti L (2007) Use of Fourier transform infrared (FT-IR) spectroscopy as a tool for pollen identification. *Aerobiologia* 23 (3):211-219

- Hesse M (2009) Pollen terminology : an illustrated handbook. Springer, Wien ; New York
- Ho R, Sziklai O (1972) On the pollen morphology of picea and tsuga species. *Grana* 12 (1):31-40. doi:10.1080/00173137209427643
- Holmes-Davis R, Tanaka CK, Vensel WH, Hurkman WJ, McCormick S (2005) Proteome mapping of mature pollen of *Arabidopsis thaliana*. *Proteomics* 5 (18):4864-4884. doi:10.1002/pmic.200402011
- Holt KA, Bennett KD (2014) Principles and methods for automated palynology. *New Phytologist* 203 (3):735-742. doi:10.1111/nph.12848
- Jardine PE, Abernethy FAJ, Lomax BH, Gosling WD, Fraser WT (2017) Shedding light on sporopollenin chemistry, with reference to UV reconstructions. *Rev Palaeobot Palyno* 238:1-6. doi:<http://doi.org/10.1016/j.revpalbo.2016.11.014>
- Jardine PE, Fraser WT, Lomax BH, Sephton MA, Shanahan TM, Miller CS, Gosling WD (2016) Pollen and spores as biological recorders of past ultraviolet irradiance. *Sci Rep-Uk* 6. doi:ARTN 39269
10.1038/srep39269
- Jiang J, Zhang Z, Cao J (2013) Pollen wall development: the associated enzymes and metabolic pathways. *Plant Biology* 15 (2):249-263. doi:10.1111/j.1438-8677.2012.00706.x
- Jiang YF, Lahlali R, Karunakaran C, Kumar S, Davis AR, Bueckert RA (2015) Seed set, pollen morphology and pollen surface composition response to heat stress in field pea. *Plant Cell Environ* 38 (11):2387-2397. doi:10.1111/pce.12589
- Joester M, Seifert S, Emmerling F, Kneipp J (2016) Physiological influence of silica on germinating pollen as shown by Raman spectroscopy. *Journal of biophotonics*. doi:10.1002/jbio.201600011
- Julier ACM, Jardine PE, Coe AL, Gosling WD, Lomax BH, Fraser WT (2016) Chemotaxonomy as a tool for interpreting the cryptic diversity of Poaceae pollen. *Rev Palaeobot Palyno* 235:140-147. doi:<http://dx.doi.org/10.1016/j.revpalbo.2016.08.004>
- Kim SS, Douglas CJ (2013) Sporopollenin monomer biosynthesis in *Arabidopsis*. *J Plant Biol* 56 (1):1-6. doi:10.1007/s12374-012-0385-3
- Klaus W (1978) On the Taxonomic Significance of Tectum Sculpture Characters in Alpine Pinus Species. *Grana* 17 (3):161-166. doi:10.1080/00173137809431961
- Lahlali R, Jiang YF, Kumar S, Karunakaran C, Liu X, Borondics F, Hallin E, Bueckert R (2014) ATR-FTIR spectroscopy reveals involvement of lipids and proteins of intact pea pollen grains to heat stress tolerance. *Frontiers in plant science* 5. doi:ARTN 747
10.3389/fpls.2014.00747
- Liang M, Zhang P, Shu X, Liu CG, Shu JN (2013) Characterization of pollen by MALDI-TOF lipid profiling. *Int J Mass Spectrom* 334:13-18. doi:10.1016/j.ijms.2012.09.007
- Lindbladh MS, O'Connor R, Jacobson GL (2002) Morphometric analysis of pollen grains for paleoecological studies: Classification of *Picea* from eastern North America. *Am J Bot* 89 (9):1459-1467. doi:DOI 10.3732/ajb.89.9.1459
- Lomax BH, Fraser WT (2015) Palaeoproxies: botanical monitors and recorders of atmospheric change. *Palaeontology* 58 (5):759-768. doi:10.1111/pala.12180
- Lomax BH, Fraser WT, Harrington G, Blackmore S, Sephton MA, Harris NBW (2012) A novel palaeoaltimetry proxy based on spore and pollen wall chemistry. *Earth Planet Sc Lett* 353:22-28. doi:10.1016/j.epsl.2012.07.039
- Lomax BH, Fraser WT, Sephton MA, Callaghan TV, Self S, Harfoot M, Pyle JA, Wellman CH, Beerling DJ (2008) Plant spore walls as a record of long-term changes in ultraviolet-B radiation. *Nat Geosci* 1 (9):592-596. doi:10.1038/ngeo278

- Lukacs R, Blumel R, Zimmermann B, Bagcoglu M, Kohler A (2015) Recovery of absorbance spectra of micrometer-sized biological and inanimate particles. *Analyst* 140. doi:10.1039/C5AN00401B
- Miller CN (1999) Implications of fossil conifers for the phylogenetic relationships of living families. *Bot Rev* 65 (3):239-277. doi:10.1007/Bf02857631
- Nakagawa T, Edouard JL, de Beaulieu JL (2000) A scanning electron microscopy (SEM) study of sediments from Lake Cristol, southern French Alps, with special reference to the identification of *Pinus cembra* and other Alpine *Pinus* species based on SEM pollen morphology. *Rev Palaeobot Palyno* 108 (1-2):1-15. doi:10.1016/S0034-6667(99)00030-5
- Nakazawa F, Uetake J, Suyama Y, Kaneko R, Takeuchi N, Fujita K, Motoyama H, Imura S, Kanda H (2013) DNA analysis for section identification of individual *Pinus* pollen grains from Belukha glacier, Altai Mountains, Russia. *Environ Res Lett* 8 (1). doi:10.1088/1748-9326/8/1/014032
- Pacini E (1996) Types and meaning of pollen carbohydrate reserves. *Sex Plant Reprod* 9 (6):362-366. doi:10.1007/Bf02441957
- Pacini E, Hesse M (2005) Pollenkitt - its composition, forms and functions. *Flora* 200 (5):399-415. doi:10.1016/j.flora.2005.02.006
- Pappas CS, Tarantilis PA, Harizanis PC, Polissiou MG (2003) New method for pollen identification by FT-IR spectroscopy. *Applied spectroscopy* 57 (1):23-27
- Parducci L, Suyama Y, Lascoux M, Bennett KD (2005) Ancient DNA from pollen: a genetic record of population history in Scots pine. *Mol Ecol* 14 (9):2873-2882. doi:10.1111/j.1365-294X.2005.02644.x
- Parodi G, Dickerson P, Cloud J (2013) Pollen Identification by Fourier Transform Infrared Photoacoustic Spectroscopy. *Applied spectroscopy* 67 (3):342-348. doi:10.1366/12-06622
- Piffanelli P, Ross JHE, Murphy DJ (1998) Biogenesis and function of the lipidic structures of pollen grains. *Sex Plant Reprod* 11 (2):65-80. doi:10.1007/s004970050122
- Pummer BG, Bauer H, Bernardi J, Chazallon B, Facq S, Lendl B, Whitmore K, Grothe H (2013) Chemistry and morphology of dried-up pollen suspension residues. *J Raman Spectrosc* 44 (12):1654-1658. doi:10.1002/jrs.4395
- Roulston TH, Cane JH, Buchmann SL (2000) What governs protein content of pollen: Pollinator preferences, pollen-pistil interactions, or phylogeny? *Ecol Monogr* 70 (4):617-643. doi:10.1890/0012-9615(2000)070[0617:Wgpcop]2.0.Co;2
- Rozema J, Broekman RA, Blokker P, Meijkamp BB, de Bakker N, van de Staaij J, van Beem A, Ariese F, Kars SM (2001) UV-B absorbance and UV-B absorbing compounds (para-coumaric acid) in pollen and sporopollenin: the perspective to track historic UV-B levels. *J Photoch Photobio B* 62 (1-2):108-117. doi:10.1016/S1011-1344(01)00155-5
- Savolainen O, Pyhajarvi T, Knurr T (2007) Gene flow and local adaptation in trees. *Annu Rev Ecol Evol S* 38:595-619. doi:10.1146/annurev.ecolsys.38.091206.095646
- Seifert S, Merk V, Kneipp J (2016) Identification of aqueous pollen extracts using surface enhanced Raman scattering (SERS) and pattern recognition methods. *Journal of biophotonics* 9 (1-2):181-189. doi:10.1002/jbio.201500176
- Seifert S, Weidner SM, Panne U, Kneipp J (2015) Taxonomic relationships of pollens from matrix-assisted laser desorption/ionization time-of-flight mass spectrometry data using multivariate statistics. *Rapid Commun Mass Sp* 29 (12):1145-1154. doi:10.1002/rcm.7207
- Shi JX, Cui MH, Yang L, Kim YJ, Zhang DB (2015) Genetic and Biochemical Mechanisms of Pollen Wall Development. *Trends in plant science* 20 (11):741-753. doi:10.1016/j.tplants.2015.07.010

- Souza CD, Kim SS, Koch S, Kienow L, Schneider K, McKim SM, Haughn G, Kombrink E, Douglas CJ (2009) A Novel Fatty Acyl-CoA Synthetase Is Required for Pollen Development and Sporopollenin Biosynthesis in *Arabidopsis*. *Plant Cell* 21 (2):507-525. doi:10.1105/tpc.108.062513
- Sowa S, Connor KF, Towill LE (1991) Temperature-Changes in Lipid and Protein-Structure Measured by Fourier-Transform Infrared Spectrophotometry in Intact Pollen Grains. *Plant Sci* 78 (1):1-9. doi:10.1016/0168-9452(91)90155-2
- Speranza A, Calzoni GL, Pacini E (1997) Occurrence of mono- or disaccharides and polysaccharide reserves in mature pollen grains. *Sex Plant Reprod* 10 (2):110-115. doi:10.1007/s004970050076
- Staszkie.J, Tyszkiew.M (1969) Natural Hybrids of *Pinus Mugo Turra* and *Pinus Silvestris L* in Nowy Targ Basin. *B Acad Pol Sci Biol* 17 (9):579-&
- Vanherpen MMA (1981) Effect of Season, Age and Temperature on the Protein Pattern of Pollen and Styles in *Petunia Hybrida*. *Acta Bot Neerl* 30 (4):277-287
- Vesprini JL, Nepi M, Cresti L, Guarnieri M, Pacini E (2002) Changes in cytoplasmic carbohydrate content during *Helleborus* pollen presentation. *Grana* 41 (1):16-20. doi:10.1080/00173130260045459
- Wachowiak W, Palme AE, Savolainen O (2011) Speciation history of three closely related pines *Pinus mugo* (T.), *P. uliginosa* (N.) and *P. sylvestris* (L.). *Mol Ecol* 20 (8):1729-1743. doi:10.1111/j.1365-294X.2011.05037.x
- Wachowiak W, Trivedi U, Perry A, Cavers S (2015) Comparative transcriptomics of a complex of four European pine species. *Bmc Genomics* 16. doi:10.1186/s12864-015-1401-z
- Watson JS, Sephton MA, Sephton SV, Self S, Fraser WT, Lomax BH, Gilmour I, Wellman CH, Beerling DJ (2007) Rapid determination of spore chemistry using thermochemolysis gas chromatography-mass spectrometry and micro-Fourier transform infrared spectroscopy. *Photoch Photobio Sci* 6 (6):689-694. doi:10.1039/b617794h
- Willis KJ, Feurdean A, Birks HJ, Bjune AE, Breman E, Broekman R, Grytnes JA, New M, Singarayer JS, Rozema J (2011) Quantification of UV-B flux through time using UV-B-absorbing compounds contained in fossil *Pinus* sporopollenin. *The New phytologist* 192 (2):553-560. doi:10.1111/j.1469-8137.2011.03815.x
- Wolkers WF, Hoekstra FA (1995) Aging of Dry Desiccation-Tolerant Pollen Does Not Affect Protein Secondary Structure. *Plant physiology* 109 (3):907-915
- Yazdani R, Lindgren D, Stewart S (1989) Gene Dispersion within a Population of *Pinus sylvestris*. *Scand J Forest Res* 4 (1-4):295-306. doi:10.1080/02827588909382567
- Yule BL, Roberts S, Marshall JEA (2000) The thermal evolution of sporopollenin. *Org Geochem* 31 (9):859-870. doi:10.1016/S0146-6380(00)00058-9
- Zhang DB, Yang XJ, Shi JX (2016) Role of lipids in plant pollen development. In: Nakamura Y (ed) *Lipids in plant and algae development*. Springer Berlin Heidelberg, New York, NY, pp 315-337
- Zimmermann B (2010) Characterization of Pollen by Vibrational Spectroscopy. *Applied spectroscopy* 64 (12):1364-1373
- Zimmermann B, Bagcioglu M, Sandt C, Kohler A (2015a) Vibrational microspectroscopy enables chemical characterization of single pollen grains as well as comparative analysis of plant species based on pollen ultrastructure. *Planta* 242 (5):1237-1250. doi:10.1007/s00425-015-2380-7
- Zimmermann B, Kohler A (2013) Optimizing Savitzky-Golay Parameters for Improving Spectral Resolution and Quantification in Infrared Spectroscopy. *Applied spectroscopy* 67 (8):892-902
- Zimmermann B, Kohler A (2014) Infrared spectroscopy of pollen identifies plant species and genus as well as environmental conditions. *Plos One* 9 (4):e95417. doi:10.1371/journal.pone.0095417

Zimmermann B, Tafintseva V, Bagcioglu M, Hoegh Berdahl M, Kohler A (2016) Analysis of Allergenic Pollen by FTIR Microspectroscopy. *Anal Chem* 88 (1):803-811. doi:10.1021/acs.analchem.5b03208

Zimmermann B, Tkalcec Z, Mesic A, Kohler A (2015b) Characterizing aeroallergens by infrared spectroscopy of fungal spores and pollen. *Plos One* 10 (4):e0124240. doi:10.1371/journal.pone.0124240

Tables

Table 1 Variability of spectral data, with values for single grain spectra and spectra based on different averaging factor, and with designated number of spectra used in the variability tests.

Type of variability	Infrared region 800-1900 cm ⁻¹ (1-PCC*) * 10 ⁻⁴			
	Single grain (200 spectra)	5 grain average (40 spectra)	10 grain average (20 spectra)	20 grain average (10 spectra)
Tsuga canadensis #1	113	24	13	7
Tsuga canadensis #2	98	23	14	8
Pinus sylvestris #1	838	251	137	67
Pinus sylvestris #2	895	296	194	120
Pinus mugo #1	662	190	101	43
Pinus mugo #2	546	165	84	47

Table 2 The PLSR coefficient of determination (R²) for differentiation between the taxa, either Pinaceae genera (*Pinus* vs *Tsuga*) or *Pinus* species (*P. sylvestris* and *P. mugo*), with the number of components in parenthesis (A_{opt} - optimal number; A_4 - four components); results are stated for different averaging factor (AF).

AF	Genera		Species	
	R ² (A_{opt})	R ² (A_4)	R ² (A_{opt})	R ² (A_4)
1	0.942 (10)	0.897	0.878 (11)	0.830
5	0.980 (9)	0.966	0.961 (6)	0.944
10	0.986 (7)	0.982	0.968 (5)	0.963
20	0.996 (6)	0.991	0.970 (4)	0.970

Figures

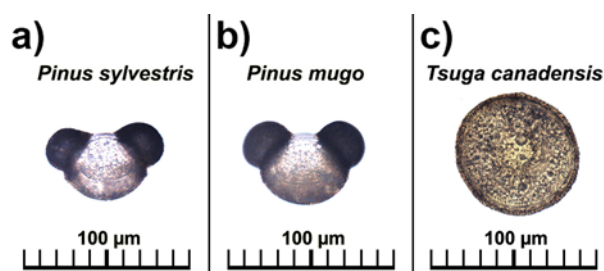


Fig. 1 Microscope image of pollens. **a** *Pinus sylvestris*, equatorial view. **b** *Pinus mugo*, equatorial view. **c** *Tsuga canadensis*, polar view

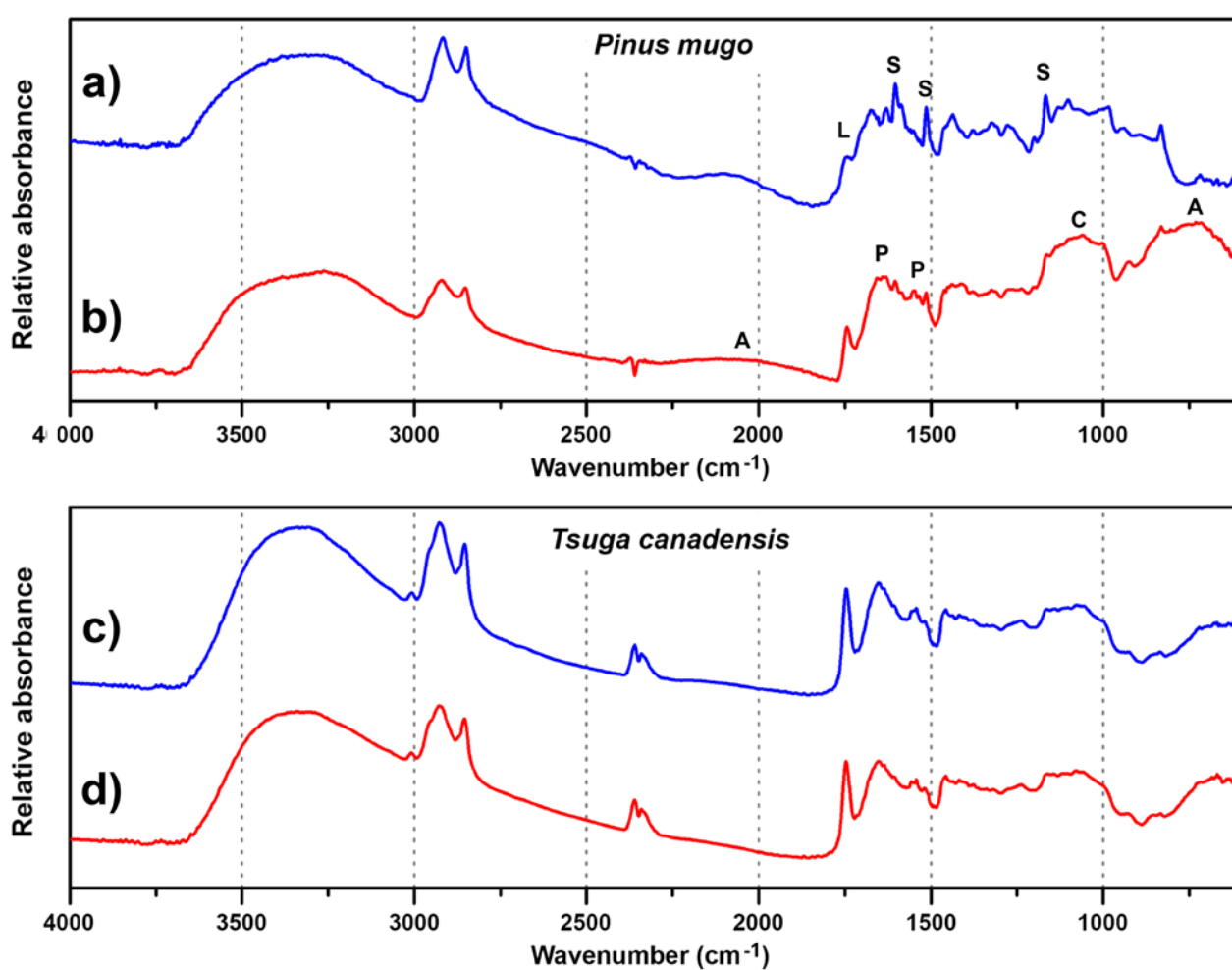


Fig. 2 FTIR microspectroscopy spectra of single pollen grains. μ FTIR spectra belonging to two *Pinus mugo* single pollen grains, one with distal polar orientation (**a**) and another with equatorial profile orientation (**b**). μ FTIR spectra belonging to two *Tsuga canadensis* single pollen grains with polar orientation (**c**, **d**). For better viewing the spectra are offset; the marked vibrational bands are associated with lipids (L), proteins (P), carbohydrates (C) and sporopollenins (S); the scattering artefacts (A) are present in **a** and **b**

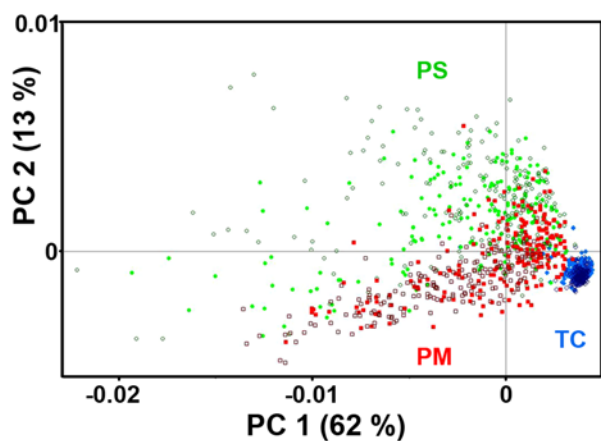


Fig. 3 PCA score plot of FTIR microspectroscopy spectral set. The set includes six samples with 200 single grain measurements per sample: *Pinus sylvestris* (PS: green, dark green), *Pinus mugo* (PM: red, dark red) and *Tsuga canadensis* (TC: blue, dark blue)

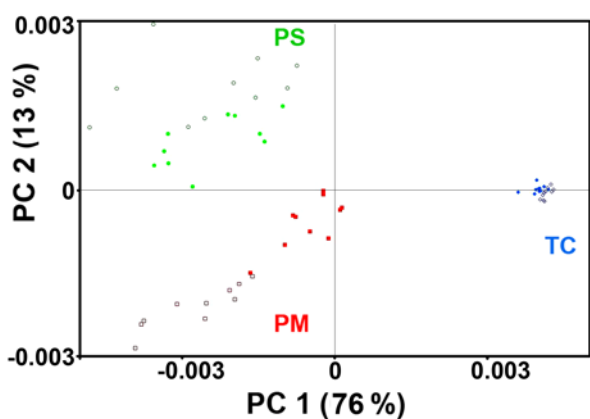


Fig. 4 PCA score plot of FTIR microspectroscopy spectral set with averaging. The set includes six samples with 10 average spectra per sample; each average spectrum is based on 20 spectra of single grains; *Pinus sylvestris* (PS: green, dark green), *Pinus mugo* (PM: red, dark red) and *Tsuga canadensis* (TC: blue, dark blue)

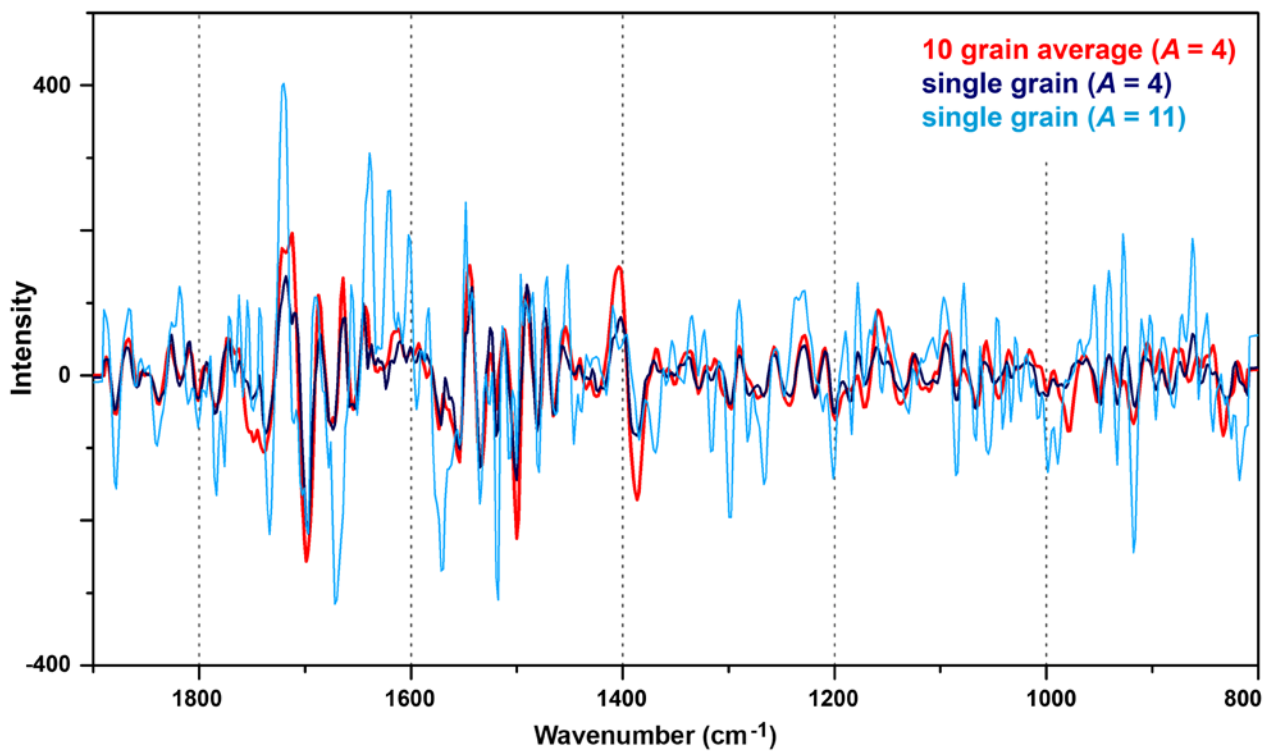


Fig. 5 Plot of PLSR regression coefficients for differentiation between *Pinus* species based on single grain and average spectra; number of components of the calibration models are designated in parenthesis